Am J Cancer Res 2022;12(2):893-906
www.ajcr.us /ISSN:2156-6976/ajcr0140863

Original Article

Decreased RNA m^{6}A methylation enhances the process of the epithelial mesenchymal transition and vasculogenic mimicry in glioblastoma

Min Tao[1*], Xiaoyu Li[1*], Lei He[1], Xiaoming Rong[1], Hongxuan Wang[1], Jingrui Pan[1], Zijing Lu[2], Xiaoni Zhang[1], Ying Peng[1,3]

[1]Department of Neurology, Sun Yat-Sen Memorial Hospital, Sun Yat-Sen University, Guangzhou 510828, Guangdong, China; [2]Department of Plastic and Cosmetic Surgery, Nanfang Hospital, Southern Medical University, Guangzhou 510510, Guangdong, China; [3]Guangdong Provincial Key Laboratory of Malignant Tumor Epigenetics and Gene Regulation, Sun Yat-Sen Memorial Hospital, Sun Yat-Sen University, Guangzhou 510828, Guangdong, China. [*]Equal contributors.

Received November 30, 2021; Accepted February 13, 2022; Epub February 15, 2022; Published February 28, 2022

Abstract: RNA N^6-methyladenosine (m^{6}A) modification is gradually thought to be an active participant in the considerable biological processes of glioblastoma (GB), providing us with a novel insight for exploring this disease. However, the role of RNA m^{6}A modification during the epithelial mesenchymal transition (EMT) or vasculogenic mimicry (VM) progression has not been investigated in GB. Here we performed a research to validate the impact exerted by AlkB homolog 5 (ALKBH5), one of "erasers" for RNA m^{6}A and methyltransferase-like 3 (METTL3) which adds m^{6}A modification to the RNAs on the progression of EMT and VM in GB. In this study, we demonstrate that the m^{6}A levels of RNAs were reduced in GB cells and glioma tissues. Patients with high mRNA expression of ALKBH5 acquired relatively shorter median overall survival (OS) time, while patients with relatively high expression of MEETL3 prolonged their disease free survival. ALKBH5 enhanced GB cell proliferation and influenced cell cycle in vitro. Decreased RNA m^{6}A methylation enhanced the progression of the EMT and VM in glioblastoma cells. ALKBH5 strengthened glioblastoma growth and enhanced the EMT and VM process of glioblastoma in vivo. Our study uncovers that RNA m^{6}A methylation suppresses the process of EMT and VM in glioblastoma, providing a new perspective to seek for a potential therapeutic target for GB.

Keywords: Glioblastoma, epithelial mesenchymal transition, vasculogenic mimicry, RNA m^{6}A methylation, ALKBH5, METTL3

Introduction

Glioblastoma (GB) is widely acknowledged as the most common malignant primary tumors in the central nervous system [1, 2]. Prevalence studies estimated that the averaged prevalence rate for malignant tumors was 42.5 per 100 000 in the United States in 2010 [3]. Despite the fact that there are some treatments for glioblastoma patients including surgery, radiotherapy and chemotherapy [4], the five-year survival rate for glioblastoma patients aged over 55 is still lower than 5% while the highest one for glioblastoma patients is no more than 25% whose age was between 0-14 [5]. Due to its invasive growth pattern and extreme advanced malignance, glioblastoma cannot be separated from normal brain tissue nearby easily and completely, which always results in its recurrence in a short time [5, 6]. Therefore, it's urgent and necessary that further investigation on the molecular mechanism of invasive growth in glioblastoma should be addressed.

The epithelial to mesenchymal transition (EMT) process is believed to equip cells with migratory and invasive properties, making cells attain the ability to initiate metastasis [7], which accounts for over 90% of cancer-associated mortality [8]. During the EMT process, loss of E-cadherin (E-Cad, CDH1) accompanied by

upregulation of N-cadherin (N-Cad, CDH2), altering cell adhesion, is thought to be a most crucial step [11]. Apart from this, the decline in extracellular matrix (ECM) protein caused by upregulation of matrix metalloproteinases (MMPs) also plays a significant role in the invasion [9, 11, 12]. Recently, an increasing amount of studies figured out that regulating EMT associated proteins, such as CDH1, CDH2 and MMPs, could modulate the migration and invasion ability of the glioblastoma, affecting the tumor progression [13-16]. Moreover, another process of vasculogenic mimicry (VM), firstly discovered in human melanoma in 1999, could surprisingly supply sufficient blood for tumors without any help from blood endothelial cells and also endow tumors with more invasive properties [17, 18]. Furthermore, several studies about VM formation in glioblastoma showed that by regulating VM in glioblastoma, tumors could also be regulated [19-21]. Therefore, more thorough studies about the EMT and VM process in glioblastoma may shed light on a novel treatment for glioblastoma.

N^6-methyladenosine (m^6A) modification, firstly reported in the 1970s [22], has been regarded to be the most abundant in eukaryotic mRNAs [23]. Identified to act an essential part in the mammalian cells [24], the process of m^6A modification is flexibly and dynamically manipulated by three categories of proteins, "writers", "erasers" and "readers" [22]. The writers consist of methyltransferase-like 3 (METTL3), METTL14 and Wilms tumor 1-associated protein (WTAP) [22, 25, 26], whereas fat mass and obesity-associated protein (FTO) and AlkB homolog 5 (ALKBH5) make up demethylases "erasers" [22, 27, 28]. And the readers, m^6A binding proteins, are comprised of YT521-B homology (YTH) domain-containing family proteins (YTHDF1/2/3), YTH domain-containing proteins (YTHDC1/2) [22, 29]. There is considerable evidence suggesting that the level of m^6A in glioblastoma could influence the proliferation, radio resistance and invasion of the tumor [30-33]. Nevertheless, only limited attention has been paid to the function of RNA m^6A modification during the progression of EMT and VM in glioblastoma.

In this study, we confirmed that the m^6A levels in RNAs decreased in glioblastoma cells and tissues. There was a distinct decline of m^6A/A ratio in U87-MG cells treated with TGF-β1. And our results indicated that overexpression of ALKBH5 and knockdown of METTL3 could promote the EMT and VM process by regulating MMP2, CDH1, CDH2 and fibronectin 1 (FN1). Thus, our study revealed that RNA m^6A modification intimately regulated the process of EMT and VM in glioblastoma.

Materials and methods

Patients

Paraffin-embedded brain tissue of 60 patients diagnosed with glioma WHO grade I to IV from 2015-2019 in Nanfang Hospital, Southern Medical University were collected, which the Institutional Ethics Committee of Sun Yat-Sen Memorial Hospital, Sun Yat-Sen University approved.

Cell culture

The human astrocyte cells HA purchased from sciencell research laboratories, USA, and the human glioblastoma multiform cells U87-MG (The STR report is displayed in the Supplementary Material) purchased from Procell Life, China, were all maintained with Dulbecco's modified Eagle medium (DMEM, GIBCO, Carlsbad, CA, USA) with 10% fetal bovine serum (FBS, BI) and 1% penicillin/streptomycin, and incubated in a humidified atmosphere of 5% CO_2 at 37°C (ThermoFisher, USA). Stable ALKBH5 overexpressing model cells and negative control cells named as ALKBH5 cells and control cells respectively were obtained by transfecting U87-MG cells with lentivirus (Ubigene, China), which were subsequently selected with puromycin (1.5 ug/ml) for 2 weeks. The expression of ALKBH5 was clarified by qPCR and western blotting. To generate METTL3 knockdown cell model, we transfected U87-MG cells with 3 different sequences of siRNA-METTL3 (The sequence is displayed in the Table S1) and negative control sequence (RiboBio, China) by lipofectamine 3000 (ThermoFisher, USA) according to the manufacturers' instructions. The most efficient sequence of siRNA-METLL3 was picked out to perform subsequent experiments, whose working concentration was 50 nM.

Immunohistochemistry (IHC)

Immunohistochemistry was performed using a standard two-step method. Briefly, 3 min of

high pressure was used to repair the antigen in citric acid buffer solution (PH=6.0). Then, the sections were incubated with endogenous peroxidase blocking buffer and normal goat serum at room temperature for 20 min, and 30 min respectively for preventing nonspecific reaction. Subsequently, the sections were incubated with ALKBH5 (Proteintech, 1:100), METTL3 (Proteintech, 1:1000), MMP2 (Bioss, 1:500), FN1 (Proteintech, 1:1000), CDH1 (Proteintech, 1:2000), and CDH2 (Proteintech, 1:5000) antibodies at 4°C overnight. After washed, the sections were subjected to the incubation with secondary antibodies, followed by treatment with the DAB chromogen. Finally, Meyer's hematoxylin used to stain the sections.

The immunoreactivity for ALKBH5 or METTL3 in glioma tissues was scored in a semi-quantitative method by evaluating intensity (0-3) and percentage of positive cells (0-4). We multiplied the intensity by percentage score as the final scores (0-12). If the final score was 0-3 or 8-12, the expression would be defined as "low" or "high" respectively. Otherwise, it would be considered as "intermediate".

Total RNA extraction and qPCR

Trizol reagent (Invitrogen, USA) was utilized to obtain the total RNA according to the manufacturer's instructions, which was then reverse-transcribed into cDNA. METTL3, ALKBH5, FN1, MMP2, CDH1 cDNA, GAPDH cDNA concentration were detected in QuantStudio 6 Flex System (ThermoFisher, USA). The comparative expression ($2^{-\Delta\Delta Ct}$) was computed by regarding GAPDH as endogenous control. Primers of targeted genes were as follow: METTL3, forward 5'-CTA TCT CCT GGC ACT CGC AAG A-3' and reverse 5'-GCT TGA ACC GTG CAA CCA CAT C-3' ALKBH5, forward 5'-GCA AGT TCC AGT TCA AGC CTA TTC G-3' and reverse 5'-TGG TAA CAC GGA GCT GCT CAG-3' FN1, forward 5'-ACA ACA CCG AGG TGA CTG AGA C-3' and reverse 5'-GGA CAC AAC GAT GCT TCC TGA G-3' MMP2, forward 5'-AGC GAG TGG ATG CCG CCT TTA A-3' and reverse 5'-CAT TCC AGG CAT CTG CGA TGA G-3' CDH1, forward 5'-GCC TCC TGA AAA GAG AGT GGA AG-3' and reverse 5'-TGG CAG TGT CTC TCC AAA TCC G-3' GAPDH, forward 5'-GTC TCC TCT GAC TTC AAC AGC G-3' and reverse 5'-ACC ACC CTG TTG CTG TAG CCA A-3'.

Western blotting

Equal amounts of protein samples were electrophoresed on SDS-polyacrylamide gel and then shifted to PVDF membranes, which was subsequently blocked using 5% BSA in TBST (50 mM Tris-HCl pH 7.4, 150 mM NaCl, and 0.05% Tween 20) at room temperature for 1 h. Next, the membranes were subjected to the incubation at 4°C overnight with primary antibodies as follows: ALKBH5 (Proteintech, 1:2000), METTL3 (Proteintech, 1:5000), MMP2 (Bioss, 1:500), FN1 (Proteintech, 1:2000), CDH1 (Proteintech, 1:2000), and CDH2 (Proteintech, 1:2000), GAPDH (Proteintech, 60004-1-Ig, 1:10,000). Horseradish peroxidase conjugated secondary antibodies, ECL (enhanced chemiluminescence) Kit (EpiZyme scientific, China) and ChemImager system (Tanon, China) were used to detect targeted proteins.

Oncomine database and gene expression profiling interactive analysis (GEPIA)

The mRNA expression of ALKBH5 and OS of 59 glioblastoma multiforme (GBM) patients were obtained from oncomine database [34]. (Data link: https://www.ncbi.nlm.nih.gov/geo/query/acc.cgi?acc=GSE4412.) Then they were divided into 3 groups according to the relative expression level of ALKBH5 mRNA, followed by the Kaplan-Meier survival analysis.

GEPIA (http://gepia.cancer-pku.cn/) whose data are based on the TCGA database was utilized to explore the correlation between ALKBH5 or METLL3 and prognostic outcomes in GBM patients. The methods were overall survival or disease free survival, while group cutoff was set as "median".

CCK-8 assay

Cells were seeded in 96-well plates at the density of 3×10^3 cells/well. After incubation at a humidified 5% CO_2 incubator at 37°C for 24 h, 48 h, 72 h and 96 h, the cell viability was measured by the CCK-8 assay according to the manufacturer's instructions.

EdU assay

Cells were seeded in 96-well plates at the density of 4×10^3 cells/well. 24 h incubation at

a humidified 5% CO_2 incubator at 37°C later, Cell-Light EdU Apollo567 In Vitro Kit were utilized to detect the proliferation ability of the cells according to the instruction (RiboBio, China).

Apoptosis assay

Cells were seeded in 6-well plates at the density of 1×10^5 cells/well. 24 h later, the cells were collected and stained with propidium iodide (PI) and Annexin V-allophycocyanin (APC). Apoptosis was evaluated by a flow cytometry analyzer.

Cell cycle staining assay

Cells were seeded in 6-well plate at the density of 2×10^5 cells/well. 24 h later, the cells were collected and stained with DNA Staining solution and Permeabilization solution. Next, a flow cytometry analyzer was utilized to measure the attribution of all stages of the cell cycle in 30 min.

RNA m^{6}A methylation quantification

The m^{6}A RNA methylation quantification kit (EpiGentek, P-9008-96, USA) was used to explore the m^{6}A/A fraction in total RNAs. The procedures were conducted according to the manufacturer's instructions, while 200 ng RNAs were fixed per assay well. The m^{6}A/A fraction was then quantified by assessing the absorbance of 450 nm on a ELX800 microplate reader (BioTek, USA).

Wound healing assay

Cells were seeded in a 6-well plate and cultured till an almost 100% confluent monolayer was shaped. Then a sterile pipette was used to scratch the cells, which were subsequently cultured in the FBS-free medium for 24 h. Then the migrating lengths were measured under a microscope (Olympus, IX73, Japan).

Invasion assay

Suspended in 200 μl FBS-free medium, 4×10^4 cells were added in the upper chamber already coated with Matrigel Matrix (Corning, 356231, USA) which was prediluted in FBS-free medium (1:5) for invading transwell kit (Corning, 3422, USA). At the same time, there would be 800 μl medium premixing with 10% FBS at the lower chamber. After 24 hours, the invaded cells were fastened and stained, the number of which were then calculated under a microscope (Olympus, BX63, Japan).

Phalloidin staining assay

F-actin Staining Kit-Red Fluorescence (abcam, ab112127, UK) was utilized to perform Phalloidin staining. The cells were seeded in 96-well plate at the density of 2×10^3 cells/well, which were then fixed, stained with Phalloidin and DAPI sequentially after 24 hours according the manufacture's protocol. Last, the cells were examined under microscope at Ex/Em = 594/610 nm.

In vitro VM tube formation assay

2.5×10^5 Cells were resuspended in FBS-free medium and added at the 24-well plates per well, which were precoated with 100 μl Matrigel Matrix and accommodated at the incubator for 1 hour. 24 h later, photos were grasped under a microscope (Olympus, IX73, Japan). The amounts of tube-like structures in five fields were calculated at random.

Animals

All animal experiments were approved by the ethics committee of Sun Yat-Sen University. BALB/C nude mice were supplied by the Guangzhou Nanfang Medical University Experimental Animal Technology Development Co., Ltd (Guangzhou, China) and were housed in a constant temperature environment (temperature: 21±2°C; humidity: 55±4%; and 12:12 h light/dark cycle). The nude mice were intracerebrally injected with U87-GFP-Luc cells (1×10^6) or U87-ALKBH5-Luc cells (1×10^6) resuspended in 5 mm^3 sterile saline to prepare the tumor-bearing nude mouse model.

CD31/34-periodic acid-Schiff (PAS) dual-staining

CD31 (1:100) (affinity, AF6191, USA) or CD34 (1:2500) (abcam, ab81289, UK) staining was similar as described in IHC before. Then Glycogen Periodic Acid Schiff (PAS/Hematoxylin) Stain Kit (Solarbio, G1281, China) was used for the PAS staining. Subsequently, the density of VM was observed by using a microscope.

Statistical analysis

Quantitative data are all represented in the form of mean ± standard deviation (SD). IBM SPSS Statistics 25.0 software was utilized to perform two-tailed student's t-test and one-way analysis of variance (ANOVA). The Kaplan-Meier method was employed to conduct survival analysis. The final scores of IHC staining were compared by Kruskal-Wallis rank sum test. And the *P* values <0.05 were thought to be statistically significant.

Results

m^{6}A levels of RNAs were reduced in GB cells and glioma tissues.

To investigate the m^{6}A levels of RNAs in GB cells, we measured the mRNA (**Figure 1A**) and protein (**Figure 1B**) expressions of ALKBH5 and METTL3 in U87-MG cells compared with HA cells, and observed that ALKBH5 was up-regulated while METTL3 was down-regulated in U87-MG cells, which indicated in GB cells m^{6}A levels of RNAs were reduced. And as expected, the m^{6}A RNA methylation quantification kit served to validate this (**Figure 1C**). We further conducted immunohistochemistry(IHC) staining with ALKBH5 and METTL3 from glioma patients ranging from WHO grade I to IV, indicating that a lower level of m^{6}A modification in RNAs was associated with a higher histopathological glioma grade (**Figure 1D**, **1E**).

We then investigated the correlation between the mRNA expression level of ALKBH5 and survival of GB patients in the oncomine database. And patients with relatively high level of mRNA expression of ALKBH5 acquired shorter OS and median OS time (7.4667 months) versus with low ALKBH5 expression (11.8667 months, *P*=0.0352) by Kaplan-Meier survival analysis (**Figure 1F**). And after exploring in the GEPIA, we only discovered that in the TCGA database GBM patients with relatively high expression of METTL3 could prolong their disease free survival compared with patients with low expression of METTL3 (**Figures 1G**, S1)

ALKBH5 enhanced GB cell proliferation and influenced cell cycle in vitro

U87-MG ALKBH5-overexpression models were established to identify its functional roles in GB. And the efficiency of the transfection was confirmed by qPCR and western blotting (Figure S2). The CCK-8 assay demonstrated that upregulation of ALKBH5 could enhance the cell viability in vitro (**Figure 2A**). In the same way, the EdU assay illustrated as well that compared with control, overexpressing ALKBH5 apparently increased the ability of cell proliferation with almost 100% elevation of ratios of EdU positive cells in U87-MG cells (**Figure 2B**, **2C**).

To investigate potential strategies by which ALKBH5 enhanced the proliferation of GB cells, we measured apoptotic rates and cell cycle distributions by the FCM analysis. Unfortunately, there was no distinct difference between U87-MG control and ALKBH5-overexpressing cells in terms of apoptotic cell rates (**Figure 2D**, **2E**). However, we found that U87-MG ALKBH5-overexpressing cells could accelerate cell cycle S phase and G2/M phase, with approximately 6% reduction of S phase and G2/M phase compared with U87-MG control cells (**Figure 2F**, **2G**). These results indicated that ALKBH5 could influence cell cycle in U87-MG cells to enhance GB cell proliferation instead of altering apoptosis.

m^{6}A levels of RNAs regulated EMT process in GB cells

First, we treated U87-MG cells with 10 ng/ml TGF-β1, which has widely been considered to be the main inducer of EMT process of cancer cells, for 2 days. Then we evaluated the difference of m^{6}A levels in RNAs between U87-MG control cells and TGF-β1 treated cells. As expected, the level of m^{6}A/A in RNAs from U87-MG cells treated with TGF-β1 was less than one tenth of that from U87-MG control cells (**Figure 3A**), which suggested that glioblastoma cells undergoing EMT process decreased m^{6}A levels of RNAs.

To further explore functions of RNA m^{6}A methylation during the EMT progression in U87-MG cells, the wound healing assay and the transwell assay were performed and we noticed that overexpression of ALKBH5 or knockdown of METTL3 (the efficiency of knockdown is displayed in the Figure S3) could both promote the migration and invasion abilities of U87-MG cells (**Figure 3B-E**). And Phalloidin staining showed that overexpression of ALKBH5 could lead to a more scattered pattern of cytoskele-

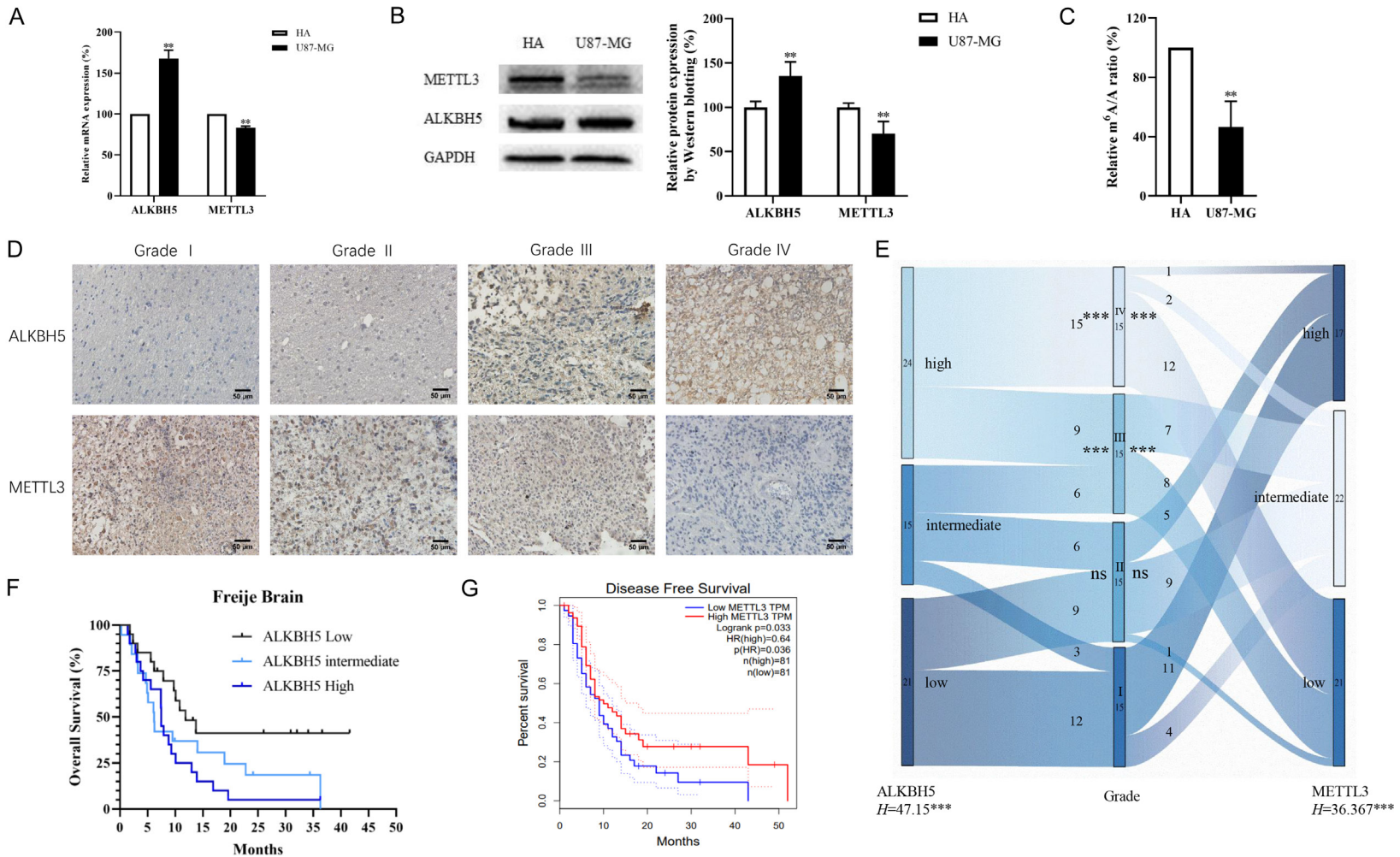

Figure 1. m^{6}A levels of RNAs were reduced in GB cells and glioma tissues. (A, B) mRNA (A) and protein (B) expressions of ALKBH5 and METTL3 in HA cells and U87-MG cells were evaluated by qPCR and western blotting, respectively. (C) The m^{6}A/A fraction in RNAs in HA and U87-MG cells were determined by the m^{6}A RNA methylation quantification kit. (D) Protein expressions of ALKBH5 and METTL3 in human glioma tissues (WHO grade I-IV) were measured by IHC (400×). (E) Sankey diagram for the final scores of IHC staining with ALKBH5 or METTL3 in glioma tissues. *H* is the Kruskal-Wallis rank sum test statistic, and the "ns" or "***" beside the node is the difference between this group and grade I group by all pairwise method. (F) Correlation between the mRNA expression of ALKBH5 and survival of GBM patients in the oncomine database. (G) Correlation between the METTL3 expression and disease free survival of GBM patients in the TCGA database from GEPIA. $^{**}P$<0.01, $^{***}P$<0.001, ns no significance. Black bar =50 μm.

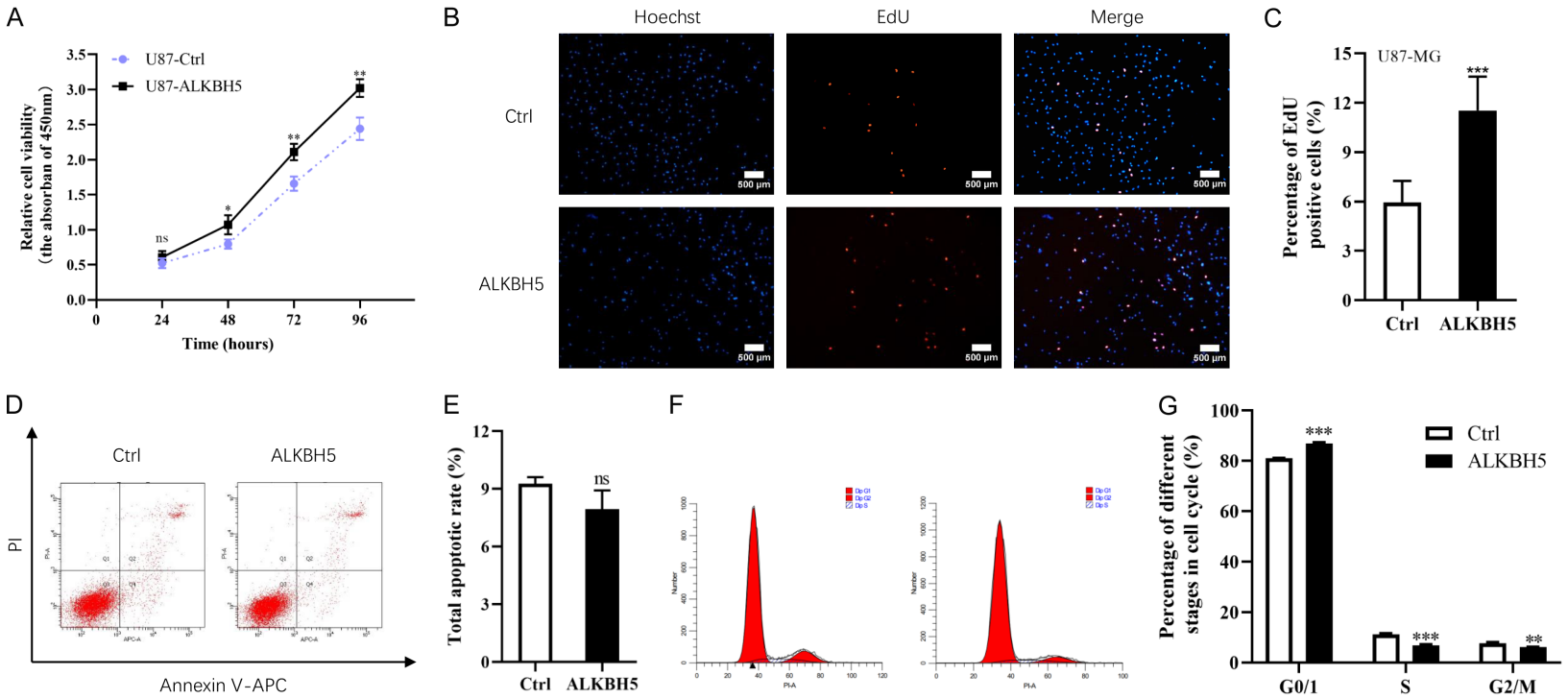

Figure 2. ALKBH5 enhanced GB cell proliferation and influenced cell cycle in vitro. (A) The viability of U87-MG control and ALKBH5 overexpression cells were measured by CCK-8 assay. (B) The proliferation of U87-MG control and ALKBH5 overexpression cells were measured by EdU assay. (D, F) The apoptosis (D) and the cell cycle (F) of U87-MG control and ALKBH5 overexpression were measured by flow cytometry. (C, E, G) statistical charts for (B, D, F) respectively. $^{*}P<0.05$, $^{**}P<0.01$, $^{***}P<0.001$, ns no significance. White bar =500 μm.

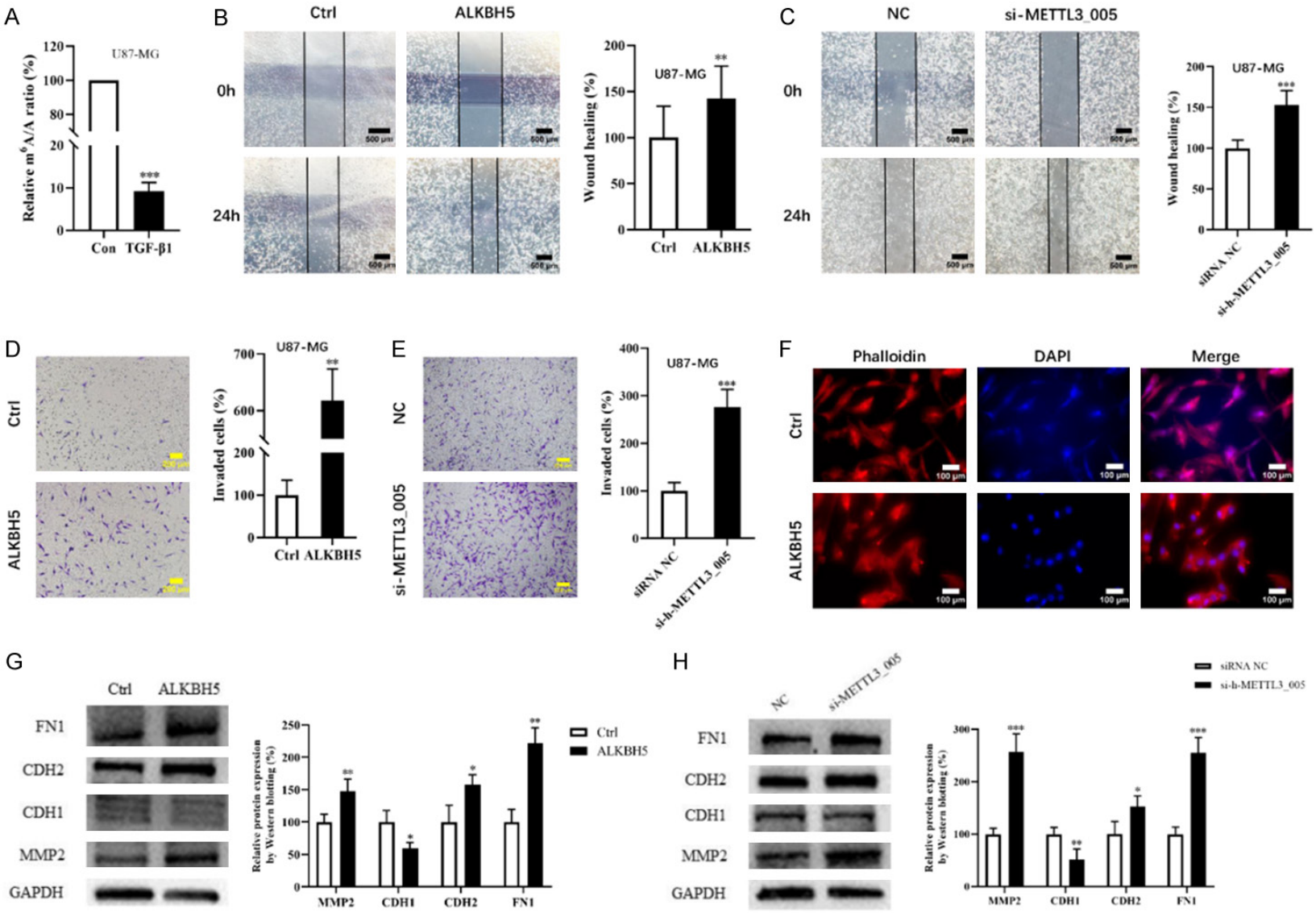

Figure 3. m^{6}A levels of RNAs regulated EMT process in GB cells. (A) The m^{6}A/A fraction in RNAs in U87-MG control and TGF-β1 treated cells were determined by the m^{6}A RNA methylation quantification kit. (B, C) Wound healing of overexpression of ALKBH5 (B) or knockdown of METTL3 (C) U87-MG cells were tracked (left) and statistically analyzed (right). (D, E) The invasion of overexpression of ALKBH5 (D) or knockdown of METTL3 (E) U87-MG cells were recorded (left) by transwell

kit and quantitatively analyzed (right). (F) Representative images of U87-MG control and ALKBH5 overexpression cells. Phalloidin was utilized to stain the cytoskeleton (F-actin), while DAPI was applied for marking the nuclei. (G, H) The protein levels of MMP2, CDH1, CDH2, and FN1 in overexpression of ALKBH5 (G) or knockdown of METTL3 (H) U87-MG cells were evaluated by Western blotting. $^{*}P<0.05$, $^{**}P<0.01$, $^{***}P<0.001$. Black bar =500 μm. Yellow bar =200 μm. White bar =100 μm.

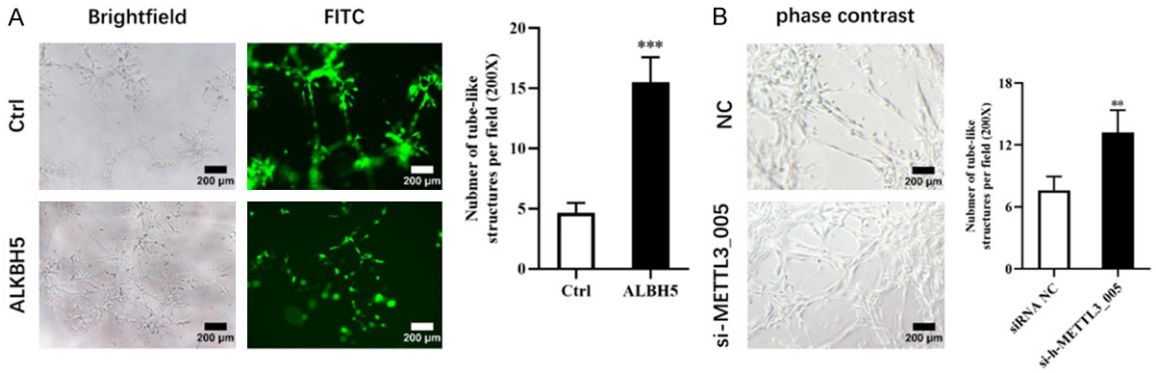

Figure 4. m^{6}A levels of RNAs regulated VM process in GB cells. (A, B) In vitro VM tube formation of upregulation of ALKBH5 (A) or knockdown of METTL3 (B) U87-MG cells were recorded (left) and statistically analyzed (right). $^{**}P<0.01$, $^{***}P<0.001$. Black or white bar =200 μm.

ton through the rearrangement of F-actin, a main protein of microfiber, which denoted a more active migrating form (**Figure 3F**).

The protein expressions of FN1, MMP2 and CDH2 were all upregulated, while the protein level of CDH1 was downregulated in ALKBH5 overexpressing or METTL3 knockdown U87-MG cells (**Figure 3G**, **3H**). These data indicated that RNA m^{6}A methylation could make a critical difference to the EMT process of glioblastoma cells.

m^{6}A levels of RNAs regulated VM process in GB cells

Moreover, to evaluate the impact of the level of RNA m^{6}A methylation on the VM of U87-MG cells, three-dimensional culture was performed. Overexpression of ALKBH5 enhanced VM formation capabilities of U87-MG cells (**Figure 4A**). Similarly, the ability of VM formation could also be up-regulated by knockdown of METTL3 in U87-MG cells (**Figure 4B**).

ALKBH5 strengthened glioblastoma growth and enhanced glioblastoma metastasis in vivo

To explore the impacts of ALKBH5 on glioblastoma in vivo, the orthotopic mouse model of U87-GFP-Luc cells were established, followed by bioluminescence imaging. We found that the tumor size of ALKBH5 overexpressing group was generally bigger than that of negative control group (**Figure 5A**), which was further validated by HE staining results (**Figure 5B**). Moreover, IHC staining with MMP2, FN1, CDH1, CDH2 were performed and we found that ALKBH5 overexpressing group had the much higher density of MMP2, FN1 and CDH2 and lower density of CDH1 than negative control group, which was the same as the results in vitro (**Figure 5C**). Unfortunately, we could not find any tube-like structures in both of groups by HE staining. Hence, we conducted CD31/34-PAS dual-staining for presenting VM from both of groups (**Figure 5D**). And interestingly, ALKBH5 overexpressing group possessed the higher VM density than the other group.

Discussion

Accumulating evidence has suggested that m^{6}A RNA modification is closely involved in progression of a rich diversity of cancers including glioblastoma [35]. In this study, we demonstrated that m^{6}A RNA modification could modulate the process of EMT and VM in glioblastoma. Briefly, m^{6}A levels of RNAs were reduced in GB cells and glioma tissues. The high level of ALKBH5 mRNA expression was correlated with the shorter survival time of the glioblastoma patients. Overexpression of ALKBH5 could enhance the proliferation of glioblastoma cells

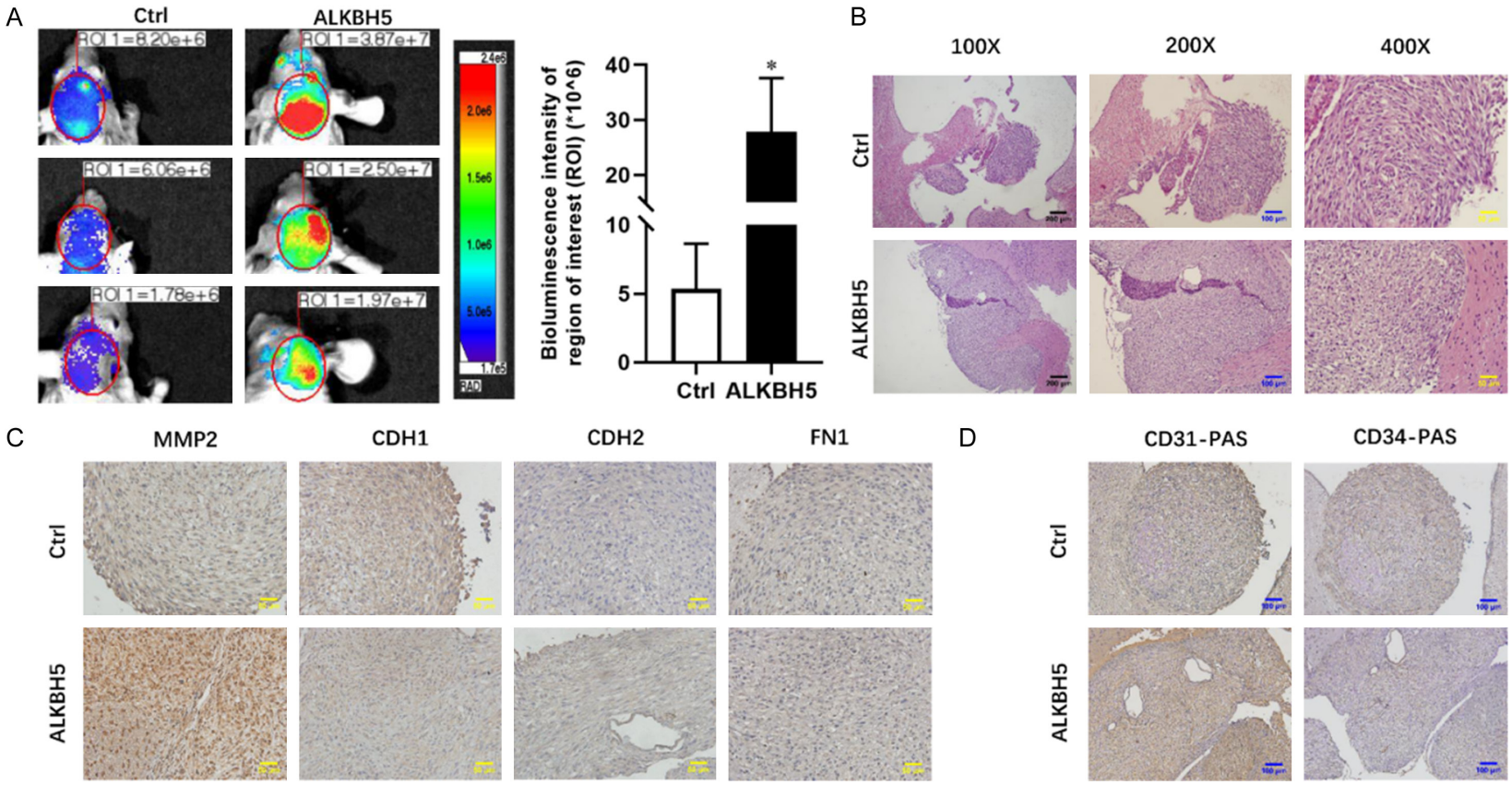

Figure 5. ALKBH5 strengthened glioblastoma growth and enhanced glioblastoma metastasis in vivo. A. Bioluminescence of luciferase-expressing-U87-MG cells in different groups of mice after injection of luciferase substrate solution and incubation for 10 min. Representative images (left) and the statistical chart (right). B. Hematoxylin-eosin staining of brain tumors in two groups. C. IHC staining with MMP2, CDH1, CDH2 and FN1 of brain tumors in two groups. D. CD31/CD34-PAS dual staining of brain tumors in two group. $^{*}P<0.05$. Yellow bar =50 μm. Blue bar =100 μm. Black bar =200 μm.

without influencing the apoptotic rates in vitro. The m^{6}A level of RNAs in glioblastoma cells undergoing EMT process declined significantly compared with the control cells. Upregulation of ALKBH5 and downregulation of METTL3 could promote the ability of migration, invasion and the process of EMT and VM by influencing the level of MMP2, CDH1, CDH2 and FN1 in glioblastoma cells. Furthermore, overexpression of ALKBH5 could also intensify the EMT and VM progression of glioblastoma in vivo.

According to our study, ALKBH5 was supposed to be a promotor of glioblastoma, while similarly METTL3 acted an anti-oncogene role in glioblastoma, which was consistent with many studies about glioblastoma. It was validated that ALKBH5 could sustain the expression of FOXM1 and maintain the cell proliferation to initiate the tumorigenicity of GB stem-like cells (GSC) by Sicong Zhang et al. [30]. Zhifeng Liu et al. reported that ALKBH5 enhanced radioresistance and invasion ability of GSC [31]. Glioblastoma had also been demonstrated to possess decreased mRNA levels of METTL3, and the growth of glioblastoma in orthotopic mice could be restrained by the knockdown of METTL3 which could also make the mice a prolonged survival [36]. Unfortunately, we could not observe distinct differences between overexpression of ALKBH5 and control glioblastoma cells in terms of apoptosis. However, it is interesting to notice that upregulation of ALKBH5 or downregulation of METTL3, which represents a relative low level of m^{6}A in RNAs, surprisingly suppress other tumors instead. For instance, Yunhao Chen et al. uncovered that in hepatocellular carcinoma cells, ALKBH5 inhabited its malignancy via suppression of LYPD1 [37]. Moreover, Dan Jin et al. revealed that in non-small cell lung cancer ALKBH5 inhibited growth and metastasis via impairing the functions of YAP [38]. Still as expected, METTL3 could promote progression in human lung cancer cells [39] and leukemia cells [40]. By contrary, METTL3 was reported to play a tumor suppressor role in renal cell carcinoma like in glioblastoma cells from our study and other studies [33, 41]. This may indicate that the function of RNA m^{6}A modification in different types of cancers varies depending on the specific environment of cells and a multitude of available downstream pathways. Totally opposite role of RNA m^{6}A modification in different tumor cells need further investigation.

Xinyao Lin et al. revealed that in HeLa, HepG2, Huh7, and A549 cells, knockout of METTL3 or upregulation of ALKBH5 inhibited EMT process through regulating the translation of Snail [42]. However, our results showed that in glioblastoma cells overexpression of ALKBH5 or downregulation of METTL3 turned out to be an inducer of EMT process, although we could not illustrate how ALKBH5 or METTL3 interact with the progression of EMT in U87-MG cells in a more detailed way, which is expected to be paid more attention to. It could be inferred that ALKBH5 or METTL3 may regulate the EMT process of U87-MG cells via changing the m^{6}A levels of CDH1, CDH2, MMP2 and FN1 mRNA which are subsequently recognized by m^{6}A binding proteins. Thus the mRNA and protein levels of CDH1, CDH2, MMP2 and FN1 alter and lead to a more invasive form, which is absolutely supposed to be clarified strictly in the future. And we are the first group to make an attempt to explore the functions of RNA m^{6}A modification during VM formation in glioblastoma, observing that a relative low level of m^{6}A in RNAs enhanced the VM progression, which is different from Kailiang Qiao et al. had presented in hepatocellular carcinoma cells [43]. Nevertheless, a more precise mechanism by which the VM progression in glioblastoma cells are modulated remains to be studied. And it should be noticed that we only observed the change in the proteins of MMP2, FN1, CDH1 and CDH2. Further studies are still needed to be conducted including what the downstream signaling of RNA m^{6}A methylation is in glioblastoma and why the role of RNA m^{6}A methylation is different between glioblastoma and other cancers.

In all, we supply evidences to clarify that decreased RNA m^{6}A methylation could enhance the process of EMT and VM in glioblastoma. Upregulation of ALKBH5 or downregulation of METTL3 strengthens the invasive properties of glioblastoma via regulating the expressions of CDH1, CDH2, MMP2 and FN1. Our work highlights the different roles of RNA m^{6}A modification in different types of cancers, further providing new insights into treatments for GB.

Acknowledgements

We are extremely appreciative of the samples of paraffin-embedded brain tissues supplied by

Prof. Xiangpeng Li (Nanfang Hospital, Southern Medical University). This work was supported by the Grant of National Key R&D Program of China, (2018YFC1314400, 2018 YFC13144-01 to Y.P), the National Natural Science Foundation of China (No. 81572481 to Y.P). and the Grant KLB09001 from the Key Laboratory of Malignant Tumor Gene Regulation and Target Therapy of Guangdong Higher Education Institutes, Sun Yat-Sen University and Grant [2013] 163 from Key Laboratory of Malignant Tumor Molecular Mechanism and Translational Medicine of Guangzhou Bureau of Science and Information Technology.

Disclosure of conflict of interest

None.

Address correspondence to: Ying Peng, Department of Neurology, Sun Yat-Sen Memorial Hospital, Sun Yat-Sen University, No. 33 Yingfeng Road, Guangzhou 510828, Guangdong, China. Tel: +86-20-3407-0569; Fax: +86-20-8133-2833; E-mail: pengy2@mail.sysu.edu.cn

References

[1] Lapointe S, Perry A and Butowski NA. Primary brain tumours in adults. Lancet 2018; 392: 432-446.

[2] Omuro A and DeAngelis LM. Glioblastoma and other malignant gliomas: a clinical review. JAMA 2013; 310: 1842-1850.

[3] Porter KR, McCarthy BJ, Freels S, Kim Y and Davis FG. Prevalence estimates for primary brain tumors in the United States by age, gender, behavior, and histology. Neuro Oncol 2010; 12: 520-527.

[4] Wick W, Osswald M, Wick A and Winkler F. Treatment of glioblastoma in adults. Ther Adv Neurol Disord 2018; 11: 1756286418790452.

[5] Ostrom QT, Gittleman H, Farah P, Ondracek A, Chen Y, Wolinsky Y, Stroup NE, Kruchko C and Barnholtz-Sloan JS. CBTRUS statistical report: primary brain and central nervous system tumors diagnosed in the United States in 2006-2010. Neuro Oncol 2013; 15 Suppl 2: ii1-56.

[6] Wen PY and Kesari S. Malignant gliomas in adults. N Engl J Med 2008; 359: 492-507.

[7] Thiery JP, Acloque H, Huang RY and Nieto MA. Epithelial-mesenchymal transitions in development and disease. Cell 2009; 139: 871-890.

[8] Chaffer CL and Weinberg RA. A perspective on cancer cell metastasis. Science 2011; 331: 1559-1564.

[9] Yilmaz M and Christofori G. EMT, the cytoskeleton, and cancer cell invasion. Cancer Metastasis Rev 2009; 28: 15-33.

[10] Wheelock MJ, Shintani Y, Maeda M, Fukumoto Y and Johnson KR. Cadherin switching. J Cell Sci 2008; 121: 727-735.

[11] Lamouille S, Xu J and Derynck R. Molecular mechanisms of epithelial-mesenchymal transition. Nat Rev Mol Cell Biol 2014; 15: 178-196.

[12] Nisticò P, Bissell MJ and Radisky DC. Epithelial-mesenchymal transition: general principles and pathological relevance with special emphasis on the role of matrix metalloproteinases. Cold Spring Harb Perspect Biol 2012; 4: a011908.

[13] Li L, Shao MY, Zou SC, Xiao ZF and Chen ZC. MiR-101-3p inhibits EMT to attenuate proliferation and metastasis in glioblastoma by targeting TRIM44. J Neurooncol 2019; 141: 19-30.

[14] Zhang G, Feng W and Wu J. Down-regulation of SEPT9 inhibits glioma progression through suppressing TGF-β-induced epithelial-mesenchymal transition (EMT). Biomed Pharmacother 2020; 125: 109768.

[15] Du X, Tu Y, Liu S, Zhao P, Bao Z, Li C, Li J, Pan M and Ji J. LINC00511 contributes to glioblastoma tumorigenesis and epithelial-mesenchymal transition via LINC00511/miR-524-5p/YB1/ZEB1 positive feedback loop. J Cell Mol Med 2020; 24: 1474-1487.

[16] Wu X, Wang Y, Yu T, Nie E, Hu Q, Wu W, Zhi T, Jiang K, Wang X, Lu X, Li H, Liu N, Zhang J and You Y. Blocking MIR155HG/miR-155 axis inhibits mesenchymal transition in glioma. Neuro Oncol 2017; 19: 1195-1205.

[17] Maniotis AJ, Folberg R, Hess A, Seftor EA, Gardner LM, Pe'er J, Trent JM, Meltzer PS and Hendrix MJ. Vascular channel formation by human melanoma cells in vivo and in vitro: vasculogenic mimicry. Am J Pathol 1999; 155: 739-752.

[18] Luo Q, Wang J, Zhao W, Peng Z, Liu X, Li B, Zhang H, Shan B, Zhang C and Duan C. Vasculogenic mimicry in carcinogenesis and clinical applications. J Hematol Oncol 2020; 13: 19.

[19] Wu HB, Yang S, Weng HY, Chen Q, Zhao XL, Fu WJ, Niu Q, Ping YF, Wang JM, Zhang X, Yao XH and Bian XW. Autophagy-induced KDR/VEGFR-2 activation promotes the formation of vasculogenic mimicry by glioma stem cells. Autophagy 2017; 13: 1528-1542.

[20] Liu Y, Li F, Yang YT, Xu XD, Chen JS, Chen TL, Chen HJ, Zhu YB, Lin JY, Li Y, Xie XM, Sun XL and Ke YQ. IGFBP2 promotes vasculogenic mimicry formation via regulating CD144 and MMP2 expression in glioma. Oncogene 2019; 38: 1815-1831.

[21] Jing F, Ruan X, Liu X, Yang C, Wang D, Zheng J, Xue Y, Shen S, Shao L, Yang Y, Wang P, Ma J and Liu Y. The PABPC5/HCG15/ZNF331 feedback loop regulates vasculogenic mimicry of glioma via STAU1-mediated mRNA decay. Mol Ther Oncolytics 2020; 17: 216-231.

[22] Lee M, Kim B and Kim VN. Emerging roles of RNA modification: m(6)A and U-tail. Cell 2014; 158: 980-987.
[23] Machnicka MA, Milanowska K, Osman Oglou O, Purta E, Kurkowska M, Olchowik A, Januszewski W, Kalinowski S, Dunin-Horkawicz S, Rother KM, Helm M, Bujnicki JM and Grosjean H. MODOMICS: a database of RNA modification pathways--2013 update. Nucleic Acids Res 2013; 41: D262-267.
[24] Wang Y, Li Y, Toth JI, Petroski MD, Zhang Z and Zhao JC. N6-methyladenosine modification destabilizes developmental regulators in embryonic stem cells. Nat Cell Biol 2014; 16: 191-198.
[25] Liu J, Yue Y, Han D, Wang X, Fu Y, Zhang L, Jia G, Yu M, Lu Z, Deng X, Dai Q, Chen W and He C. A METTL3-METTL14 complex mediates mammalian nuclear RNA N6-adenosine methylation. Nat Chem Biol 2014; 10: 93-95.
[26] Ping XL, Sun BF, Wang L, Xiao W, Yang X, Wang WJ, Adhikari S, Shi Y, Lv Y, Chen YS, Zhao X, Li A, Yang Y, Dahal U, Lou XM, Liu X, Huang J, Yuan WP, Zhu XF, Cheng T, Zhao YL, Wang X, Rendtlew Danielsen JM, Liu F and Yang YG. Mammalian WTAP is a regulatory subunit of the RNA N6-methyladenosine methyltransferase. Cell Res 2014; 24: 177-189.
[27] Jia G, Fu Y, Zhao X, Dai Q, Zheng G, Yang Y, Yi C, Lindahl T, Pan T, Yang YG and He C. N6-methyladenosine in nuclear RNA is a major substrate of the obesity-associated FTO. Nat Chem Biol 2011; 7: 885-887.
[28] Zheng G, Dahl JA, Niu Y, Fedorcsak P, Huang CM, Li CJ, Vågbø CB, Shi Y, Wang WL, Song SH, Lu Z, Bosmans RP, Dai Q, Hao YJ, Yang X, Zhao WM, Tong WM, Wang XJ, Bogdan F, Furu K, Fu Y, Jia G, Zhao X, Liu J, Krokan HE, Klungland A, Yang YG and He C. ALKBH5 is a mammalian RNA demethylase that impacts RNA metabolism and mouse fertility. Mol Cell 2013; 49: 18-29.
[29] Zhao Y, Shi Y, Shen H and Xie W. m(6)A-binding proteins: the emerging crucial performers in epigenetics. J Hematol Oncol 2020; 13: 35.
[30] Zhang S, Zhao BS, Zhou A, Lin K, Zheng S, Lu Z, Chen Y, Sulman EP, Xie K, Bögler O, Majumder S, He C and Huang S. m(6)A demethylase ALKBH5 maintains tumorigenicity of glioblastoma stem-like cells by sustaining FOXM1 expression and cell proliferation program. Cancer Cell 2017; 31: 591-606, e596.
[31] Kowalski-Chauvel A, Lacore MG, Arnauduc F, Delmas C, Toulas C, Cohen-Jonathan-Moyal E and Seva C. The m^6A RNA demethylase ALKBH5 promotes radioresistance and invasion capability of glioma stem cells. Cancers (Basel) 2020; 13: 40.
[32] Liu Z, Chen Y, Wang L and Ji S. ALKBH5 promotes the proliferation of glioma cells via enhancing the mRNA stability of G6PD. Neurochem Res 2021; 46: 3003-3011.
[33] Ji JW, Zhang YD, Lai YJ and Huang CG. Mettl3 regulates the proliferation, migration and invasion of glioma cells by inhibiting PI3K/Akt signaling pathway. Eur Rev Med Pharmacol Sci 2020; 24: 3818-3828.
[34] Freije WA, Castro-Vargas FE, Fang Z, Horvath S, Cloughesy T, Liau LM, Mischel PS and Nelson SF. Gene expression profiling of gliomas strongly predicts survival. Cancer Res 2004; 64: 6503-6510.
[35] Xiang Y, Laurent B, Hsu CH, Nachtergaele S, Lu Z, Sheng W, Xu C, Chen H, Ouyang J, Wang S, Ling D, Hsu PH, Zou L, Jambhekar A, He C and Shi Y. RNA m(6)A methylation regulates the ultraviolet-induced DNA damage response. Nature 2017; 543: 573-576.
[36] Visvanathan A, Patil V, Arora A, Hegde AS, Arivazhagan A, Santosh V and Somasundaram K. Essential role of METTL3-mediated m(6)A modification in glioma stem-like cells maintenance and radioresistance. Oncogene 2018; 37: 522-533.
[37] Chen Y, Zhao Y, Chen J, Peng C, Zhang Y, Tong R, Cheng Q, Yang B, Feng X, Lu Y, Xie H, Zhou L, Wu J and Zheng S. ALKBH5 suppresses malignancy of hepatocellular carcinoma via m(6)A-guided epigenetic inhibition of LYPD1. Mol Cancer 2020; 19: 123.
[38] Jin D, Guo J, Wu Y, Yang L, Wang X, Du J, Dai J, Chen W, Gong K, Miao S, Li X and Sun H. m(6)A demethylase ALKBH5 inhibits tumor growth and metastasis by reducing YTHDFs-mediated YAP expression and inhibiting miR-107/LATS2-mediated YAP activity in NSCLC. Mol Cancer 2020; 19: 40.
[39] Lin S, Choe J, Du P, Triboulet R and Gregory RI. The m(6)A methyltransferase METTL3 promotes translation in human cancer cells. Mol Cell 2016; 62: 335-345.
[40] Vu LP, Pickering BF, Cheng Y, Zaccara S, Nguyen D, Minuesa G, Chou T, Chow A, Saletore Y, MacKay M, Schulman J, Famulare C, Patel M, Klimek VM, Garrett-Bakelman FE, Melnick A, Carroll M, Mason CE, Jaffrey SR and Kharas MG. The N(6)-methyladenosine (m(6)A)-forming enzyme METTL3 controls myeloid differentiation of normal hematopoietic and leukemia cells. Nat Med 2017; 23: 1369-1376.
[41] Li X, Tang J, Huang W, Wang F, Li P, Qin C, Qin Z, Zou Q, Wei J, Hua L, Yang H and Wang Z. The M^6A methyltransferase METTL3: acting as a tumor suppressor in renal cell carcinoma. Oncotarget 2017; 8: 96103-96116.

[42] Lin X, Chai G, Wu Y, Li J, Chen F, Liu J, Luo G, Tauler J, Du J, Lin S, He C and Wang H. RNA m(6)A methylation regulates the epithelial mesenchymal transition of cancer cells and translation of Snail. Nat Commun 2019; 10: 2065.

[43] Qiao K, Liu Y, Xu Z, Zhang H, Zhang H, Zhang C, Chang Z, Lu X, Li Z, Luo C, Liu Y, Yang C and Sun T. RNA m^6A methylation promotes the formation of vasculogenic mimicry in hepatocellular carcinoma via Hippo pathway. Angiogenesis 2021; 24: 83-96.

Table S1. Sequences of siRNAs

Code	Name	Sequence (5'-3')
siG151008053209	si-h-METTL3_005	GCAAGAATTCTGTGACTAT
siG151229110222	si-h-METTL3_008	AACTTGCCCAAGATACTGA
siG151229110235	si-h-METTL3_009	AACAATGGATTGTTCCTTG

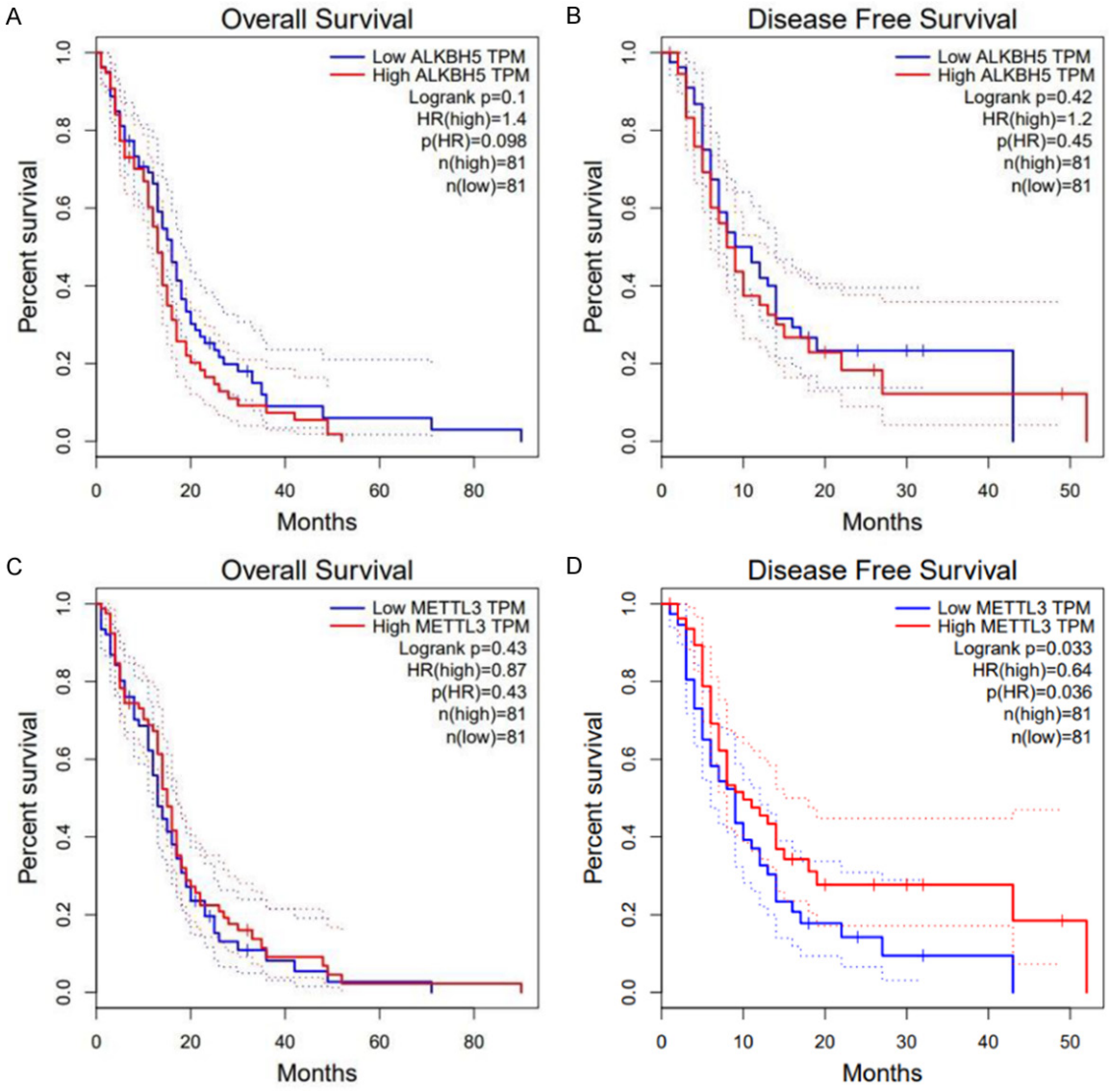

Figure S1. The correlation between ALKBH5 or METTL3 expression and prognostic outcome in GBM patients from the TCGA database by employing GEPIA. A, C. Overall survival for ALKBH5 and METTL3, respectively. B, D. Disease free survival for ALKBH5 and METTL3, respectively.

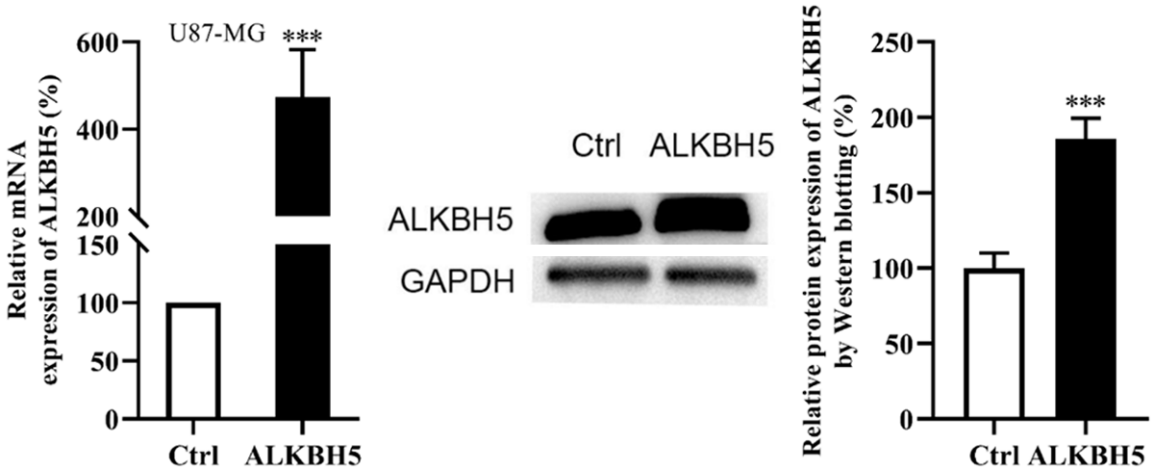

Figure S2. mRNA and protein expressions of ALKBH5 in control and ALKBH5 U87-MG cells were measured by qRT-PCR and western blot analysis, respectively. ***P<0.001.

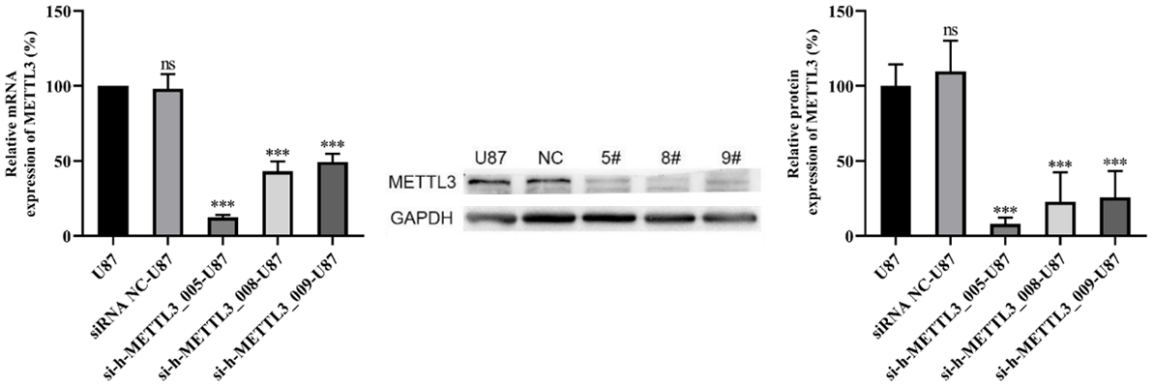

Figure S3. mRNA and protein expressions of METTL3 in U87-MG cells and U87-MG cells transfected with siRNA NC or different siRNA-h-METTL3 were measured by qRT-PCR and Western blotting, respectively. ns no significance, ***P<0.001 by Dunnett-t test.